1-1-1996

Experimental and Theoretical Investigation of Recombination Pumped X-ray Lasers Driven by High-Intensity, Short Pulse Lasers

Thomas D. Donnelly
Harvey Mudd College

L. Da Silva
Lawrence Livermore National Laboratory

R. W. Lee
Lawrence Livermore National Laboratory

S. Mrowka
Lawrence Livermore National Laboratory

M. Hofer
University of California - Berkeley

See next page for additional authors

Experimental and theoretical investigation of recombination-pumped x-ray lasers driven by high-intensity, short-pulse lasers

T. D. Donnelly*

Department of Physics, University of California, Berkeley, Berkeley, California 94720

L. Da Silva, R. W. Lee, and S. Mrowka

Lawrence Livermore National Laboratory, Livermore, California 94550

M. Hofer and R. W. Falcone

Department of Physics, University of California, Berkeley, Berkeley, California 94720

Received March 9, 1995; revised manuscript received June 7, 1995

We have experimentally investigated a recombination-pumped soft-x-ray laser on a Lyman-α transition (135 Å) of hydrogenlike lithium. Furthermore, we have modeled the dynamics of this system, including the effects of the multipeaked electron distribution function that is obtained from the sequential, optical-field ionization of an atom. We compare the predictions of our model and our experimental results. © 1996 Optical Society of America

The generation of recombination-pumped x-ray laser systems has gained new interest with the development of high-intensity, short-pulse lasers.[1,2] Recombination-pumped laser systems require electron–ion recombination to occur on a time scale that is short compared with the natural lifetime of the laser transition, thus requiring a plasma with a high electron density n_e and a cold-electron temperature T_e.

High-intensity, ultrashort-pulse lasers ionize atoms in a regime in which the resulting free-electron energies can be predicted by a quasi-static-field, tunneling-ionization model.[1,3,4] Under such conditions, sequential optical-field ionization (OFI) results in multiply charged ions and in a multiply peaked electron energy distribution. The strong dependence on electron energy of the three-body electron-ion recombination cross section makes the successful high-gain operation of a recombination-pumped laser dependent on the presence of low-energy electrons.[5–7] OFI of weakly bound electrons yields such electrons; however, higher-energy electrons, generated by ionization of electrons that are more tightly bound, limit laser gain in two ways. First, high-energy electrons inhibit the cascade of excited-state population to the upper laser level; and, second, these electrons collisionally heat colder electrons.

Nagata *et al.*[8] have reported gain at 135 Å on the Lyman-α transition of Li^{2+}. In this experiment Li metal was ablated from a solid target by a relatively low-intensity laser pulse. The resulting plasma plume was then irradiated by a high-intensity, short-pulse laser, which generated Li^{3+} (see Fig. 1 of Ref. 8 for the experimental setup). Subsequent recombination of Li^{3+} with cold electrons was proposed as the pumping mechanism of the laser transition. In this paper we present our experimental investigation of the Li system and compare our findings with the results of the modeling of the system's dynamics that was described in a previous paper.[9] We summarize the results of the modeling below.

The fully ionized Li plasma will initially contain three distinguishable electron distributions: one cold and two hot. Under experimental conditions similar to our own (as in Ref. 8), we laser ablate Li metal to form the vapor that is irradiated by the high-intensity pump pulse), the cold-electron distribution was measured to have a temperature of the order of 1 eV; the electron density in this experiment was estimated to be 2×10^{17} cm^{-3}.[8] The hot-electron distributions result from sequential OFI of Li^{1+} and Li^{2+} by the pump pulse. For example, using the quasi-static-field tunneling model,[1,4] we calculate that the electron distributions will have temperatures T_e(OFI) of 25 and 140 eV when they are produced by a 400-nm linearly polarized 125-fs pump pulse with a peak intensity of 2×10^{17} W/cm^2 (typical values in our experiment).

The modeling in this paper is carried out with the atomic and plasma physics kinetics code FLY, which was described in a previous paper.[9] In the same paper, cooling of the Li plasma filament was considered after the initial ionization heating; the temperatures of the three electron distributions did not change significantly on the time scale of gain (approximately 10 ps) in the system. Gain on the Lyman-α transition was computed assuming linear Stark broadening of the gain cross section.[2]

We first consider the effect of the OFI electrons on gain that can be achieved on the Lyman-α transition. Figure 1 shows the calculated peak gain for T_e(cold) = 1 eV as a function of T_e(OFI) for a variety of ion densities, n_{ion}. We assume for simplicity that both OFI electrons have the same temperature, and we vary this T_e(OFI)

0740-3224/96/010185-04$06.00

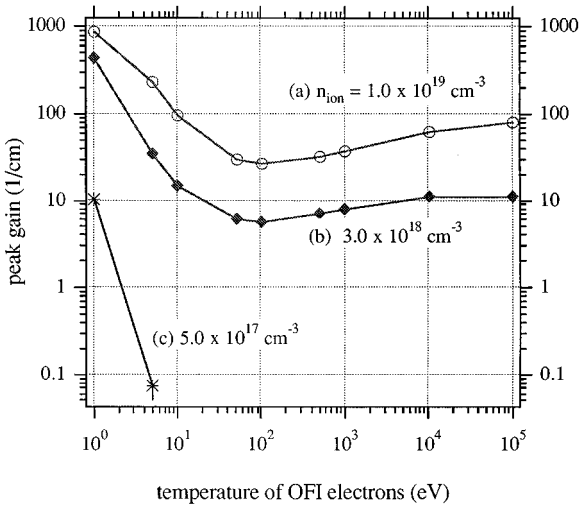

Fig. 1. Peak gain on the Lyman-α transition in Li^{2+} as a function of the OFI electron temperature. The cold-electron temperature [T_e(cold)] is held constant at 1 eV, and $(1/2)n_e$(OFI) = n_e(cold) = $n_{\rm ion}$. (a) $n_{\rm ion} = 1.0 \times 10^{19}$ cm^{-3}, (b) $n_{\rm ion} = 3.0 \times 10^{18}$ cm^{-3}, (c) $n_{\rm ion} = 5.0 \times 10^{17}$ cm^{-3}. This figure is taken from Ref. 9.

value from 1 eV to 100 keV. Based on this figure, the ion densities used in this analysis will be higher than those reported in Ref. 8.

Three regions of interest can be discerned in Fig. 1: the relatively high gain regions at the lowest and highest OFI electron temperature and a region of lower gain near temperatures of 100 eV. The three-body electron–ion recombination rate (for a single electron distribution) summed over all the levels is given by[7]

$$R_{\rm three-body}(\rm s^{-1}) = \frac{1.8 \times 10^{-8} Z^3 {n_e}^2 \ln(\Lambda)}{{T_e}^{9/2}}, \qquad (1)$$

where T_e(K) is the electron temperature, Z is the ion charge state, n_e (cm^{-3}) is the electron density, and $\ln(\Lambda)$ is the Coulomb logarithm. At low OFI electron temperatures gain is high because of rapid recombination [Eq. (1)] and the enhanced collisional cascade of population to the lowest excited state (and the upper laser state), $n = 2$ in Li^{2+}.[6] High values of T_e(OFI) also result in relatively large gain because the OFI electrons essentially decouple from the system.

In the region of T_e(OFI) $\approx$ 100 eV (compared with colder temperatures), the OFI electrons will reduce three-body recombination. Additionally, they retard the collisional cascade of population to $n = 2$ because, in this range of T_e(OFI), intralevel collisions tend to establish a distribution within the entire manifold of excited Li^{2+} states; in the steady state this distribution would become a Boltzmann distribution characterized by T_e(OFI). Thus gain is reduced compared with that in the case of colder or hotter OFI electrons.

Figure 1 also illustrates the strong dependence of gain on ion density. As the ion density drops from 1.0×10^{19} cm^{-3} [curve (a)] to 3.0×10^{18} cm^{-3} [curve (b)] to 5.0×10^{17} cm^{-3} [curve (c)] reduced gain results from the decreased three-body and collisional de-excitation rates at lower electron densities and from the decreased number of ions that are radiating.

Gain in recombination-pumped systems decreases sharply with increasing T_e. In the Li system, gain depends most strongly on the value of cold-electron temperature; this temperature will increase from its initial value through a variety of processes.[9] First, the cold- and the hot-electron distributions will equilibrate, causing an increase in the value of T_e(cold).[10] Second, recombination heating of the cold-electron population will occur as Li^{2+} is formed. Third, collisional de-excitation of electrons in excited states of the Li^{2+} ion (three-body recombination favors recombination to excited states of an ion[7]) will result in further heating of the cold-electron population.

All the above processes serve to reduce the achievable gain in the Li system; we can compensate for this reduction in gain only by increasing the Li^{2+} ion density, and hence the electron density, to maintain fast recombination and collisional deexcitation. Experimentally, however, high ion density presents a problem for the formation of a long x-ray laser channel in the plasma.

Demonstrable high gain in the Li system is limited by the pump laser's ability to ionize and to penetrate a high-density plasma.[11,12] A focused, Gaussian laser pulse has its highest intensity on axis; this causes a target gas to be ionized to a higher charge state on axis than in regions extending radially outward. The plasma created by this laser pulse will have an electron density profile that matches the laser's intensity profile and, therefore, a refractive-index profile that causes the plasma to refract, or to defocus, the incident laser.

A pump pulse subjected to this defocusing will be kept from reaching the peak focused intensity expected in a plasma-free region. In addition the plasma channel created will be shorter than expected.[12] In practice, this means that a relatively short length of plasma is ionized to the desired charge state (the state required for operation of the x-ray laser), and therefore a shorter gain–length product will result. This causes the intensity of the x-ray laser emission to be exponentially smaller than expected.

An estimate of the electron density difference δn_e (on-axis density minus off-axis density) that a laser can suffer across its spatial profile before being defocused is given by[11]

$$\delta n_e / n_c = \lambda^2 / (\pi \omega_0)^2, \qquad (2)$$

where n_c is the critical density of the plasma at the laser wavelength λ and ω_0 is the $1/e$ radius of the laser's field amplitude at focus. For a fixed focal geometry a shorter laser wavelength will permit penetration to higher plasma density (recall that n_c varies as the inverse square of the wavelength); a higher-density plasma results in a higher-gain recombination-pumped laser system (see Fig. 1).

Figure 2 shows the Lyman-α transition emission as a function of plasma length in our experiment. In the experiment we irradiate a Li vapor with either an 800- or a 400-nm-wavelength pump pulse and, using a streak camera, look at the resulting plasma's on-axis Lyman-α emission. An 800-nm-wavelength pump pulse results in a total emission strength that is independent of plasma length. When the plasma is irradiated by a 400-nm-wavelength pump pulse the signal is seen to grow nonlinearly before saturating at longer plasma lengths.

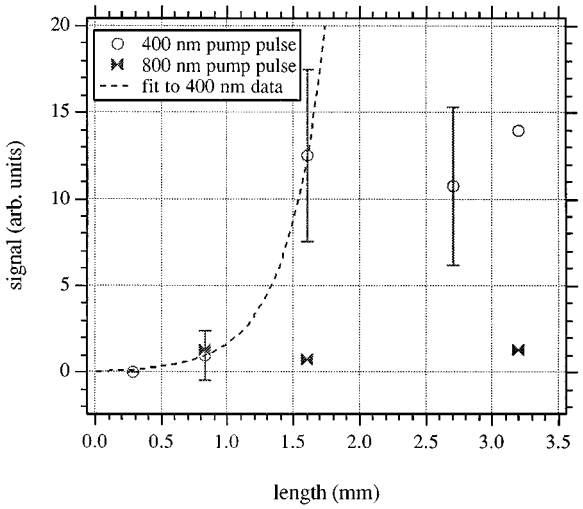

Fig. 2. Signal at the Lyman-α transition wavelength as a function of plasma length. The error bars indicate the standard deviation of the signal level computed from multiple shots. The dashed curve is a fit to the 400-nm-wavelength pump-pulse data at short plasma lengths, indicating a gain of 35 cm^{-1}.

These results yield information about the plasma density. The Li vapor in this experiment is of a high enough density that the 800-nm pump pulse is defocused within the first millimeter of plasma length. This result is implied by the Lyman-α emission data and was verified by imaging of the 800-nm pulse *in situ*. For the experimental conditions under which the 800-nm data of Fig. 2 were obtained ($\omega_0 \approx 25$ μm), Eq. (2) implies that $\delta n_e > 10^{17}$ cm^{-3}, because the pulse was quickly defocused by the plasma. For the 400-nm pump pulse, which penetrates the plasma a distance of less than one confocal parameter, Eq. (2) indicates a δn_e at, or above, 10^{18} cm^{-3} ($\omega_0 \approx 12$ μm). We take δn_e to be equal to n_{ion} because the first electron in Li is removed at very low pump-pulse intensity and forms a spatially uniform charge background.

Figure 2 shows a fit[13] of 35 cm^{-1} to the short plasma length, 400-nm pump-pulse data. Figure 1 indicates that an ion density of 3.0×10^{18} cm^{-3} would result in a gain of roughly 10 cm^{-1} for $T_e(\mathrm{cold}) = 1$ eV and $T_e(\mathrm{OFI}) \approx 100$ eV. This is approximately $T_e(\mathrm{OFI})$ (see above) and n_{ion} for our experimental conditions. This $T_e(\mathrm{cold})$ value should be taken as a lower limit for two reasons. First, when neutral Li is singly ionized by the low-intensity, leading edge of the pump pulse (400 nm), two-photon ionization leaves the free electron with a residual energy of 1 eV. Second, the collisional heating processes discussed above will quickly bring the electron temperature above 1 eV.[9]

By studying the time history of the Lyman-α transition fluorescence we can put an upper limit on $T_e(\mathrm{cold})$ and thus bracket the gain value that we predict for our system. We can then compare this prediction with the measured gain value to check our model's accuracy.

In Fig. 3 the time history of the Lyman-α transition fluorescence is shown for the conditions of Fig. 2 (400-nm pump pulse). The rise time of the Lyman-α signal is limited by the time resolution of our streak camera (approximately 15 ps). The fall time, however, is well fitted by an exponential decay with a time constant of 26 ps (the lifetime of the Lyman-α transition). This indicates that the majority of the electron population reaches the $n = 2$ state on a time that is less than 26 ps.

The electrons that ultimately reach the upper state of the Lyman-α transition ($n = 2$) have undergone three-body recombination and collisional de-excitation from an upper Li^{2+} state. At $n_e(\mathrm{cold}) = 3.0 \times 10^{18}$ cm^{-3}, three-body recombination is the bottleneck in this process. If three-body recombination is the slowest of the processes that the electron undergoes in reaching the $n = 2$ state, and it takes the electron less than 26 ps to reach that state, we can put an upper limit on the electron temperature, using Eq. (1). Taking the cold-electron density to be 3.0×10^{18} cm^{-3}, a three-body recombination time of 26 ps implies that $T_e(\mathrm{cold}) = 3$ eV. This value is consistent with the collisional heating discussed in Ref. 9, where it was shown that $T_e(\mathrm{cold})$ rapidly reaches a temperature of a few electron volts in the Li system.

Knowing the approximate n_{ion} and $T_e(\mathrm{cold})$ values, we can make a prediction for the gain of our system. We expect the gain to be 1–10 cm^{-1} for $T_e(\mathrm{cold})$ between 3 and 1 eV.[9] This range of gain is below the measured value but gives reasonable agreement with the data.

Although we were unable to demonstrate experimentally a large gain–length product (owing to ionization defocusing in the high-density Li plasma), we developed a model that gives a comprehensive understanding of the dynamics of the Li system. With the inclusion of collisional heating, we developed a consistent picture of the physical processes in a recombination-pumped system, and furthermore, we were able to check the model's validity through the application of experimental parameters.

For comparison, we calculate that the peak gain of the Li system with an ion density of 1×10^{19} cm^{-3}, $T_e(\mathrm{cold}) =$ 1 eV, and $T_e(\mathrm{OFI}) = 40$, 200 eV will be 10 cm^{-1} when collisional heating of the cold-electron distribution is included, as discussed above (compare with Fig. 1, in which collisional heating is excluded). This gain would require a plasma filament of greater than 1-cm length to reach saturation of the laser transition. A KrF laser (desirable because of its short wavelength, 248 nm) would require a focused spot size of 20 μm to achieve a confocal parame-

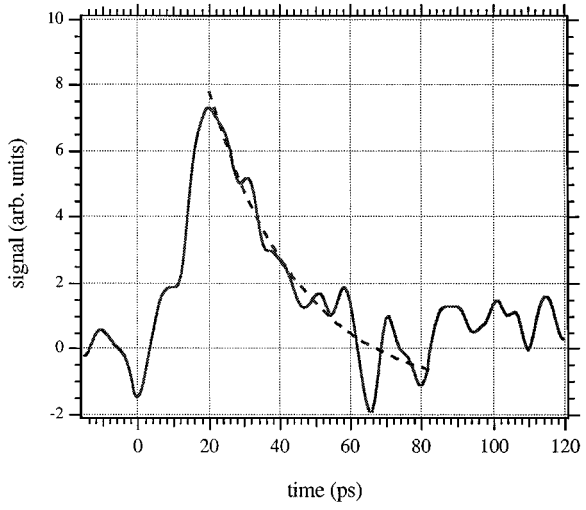

Fig. 3. Time history of the signal at the Lyman-α transition wavelength. The dashed curve indicates the falloff of an exponential with a time constant of 26 ps.

ter of 1 cm; from Eq. (2) this spot size will allow a plasma with a density of only 3×10^{17} cm^{-3} to be penetrated. A large gain–length product, therefore, will be difficult to achieve in the Li system unless the effects of plasma defocusing can be overcome in a light-guided system.

Experimental demonstration of a Li system with higher gain, or with a larger gain–length product, will require methods of coupling high-intensity, short-pulse lasers into plasmas with high ion density ($>10^{19}$ cm^{-3}). The fact that achieving high gain in the Li system calls for relatively high ion density results from the consideration of collisional heating of the cold electrons and the interaction of hotter, OFI electrons with the lasing ions. This conclusion is in conflict with the ion densities reported in Ref. 8; further research will be necessary to resolve the discrepancy.

ACKNOWLEDGMENTS

The authors acknowledge helpful discussions with Ernie Glover and David Eder. This research was supported by the U.S. Air Force Office of Scientific Research and through a collaboration with Lawrence Livermore National Laboratory under contract W-7405-ENG-48.

*Present address, Department of Physics, Swarthmore College, Swarthmore, Pennsylvania 19081.

REFERENCES

1. N. H. Burnett and P. B. Corkum, J. Opt. Soc. Am. B **6**, 1195 (1989); P. B. Corkum, N. H. Burnett, and F. Brunel, Phys. Rev. Lett. **62,** 1259 (1989).
2. N. H. Burnett and G. D. Enright, J. Quantum Electron. **26,** 1797 (1990).
3. T. E. Glover, T. D. Donnelly, E. A. Lipman, A. Sullivan, and R. W. Falcone, Phys. Rev. Lett. **73,** 78 (1994).
4. M. V. Ammosov, N. B. Delone, and V. P. Krainov, Sov. Phys. JETP **64,** 1191 (1986).
5. E. Hinnov and J. Hirschberg, Phys. Rev. **125**, 795 (1962); W. Lotz, Z. Phys. **216,** 241 (1968).
6. G. J. Pert, J. Phys. B **23,** 619 (1990).
7. Y. Zel'Dovich and Y. Raizer, in *Physics of Shock Waves and High-Temperature Hydrodynamic Phenomena,* W. Hayes and R. Probestein, eds. (Academic, New York, 1966), pp. 406–413.
8. Y. Nagata, K. Midorikawa, S. Kubodera, M. Obara, H. Tashiro, and K. Toyoda, Phys. Rev. Lett. **71,** 3774 (1993).
9. T. D. Donnelly, R. W. Lee, and R. W. Falcone, Phys. Rev. A **51,** 2691 (1995).
10. L. Spitzer, *Physics of Fully Ionized Gases* (Interscience, New York, 1962), pp. 131–136.
11. R. Rankin, C. E. Kapjack, N. H. Burnett, and P. B. Corkum, Opt. Lett. **16,** 835 (1991); for a potential solution to this problem see C. G. Durfee III and H. M. Milchberg, Phys. Rev. Lett. **71,** 2409 (1993).
12. A. Sullivan, H. Hamster, S. P. Gordon, and R. W. Falcone, Opt. Lett. **19,** 1544 (1994).
13. R. C. Elton, *X-ray Lasers* (Academic, San Diego, Calif., 1990), p. 21.